Mol Neurobiol (2012) 45:488–498
DOI 10.1007/s12035-012-8272-y

A New Trend in the Experimental Methodology for the Analysis of the Thioflavin T Binding to Amyloid Fibrils

Irina M. Kuznetsova · Anna I. Sulatskaya · Vladimir N. Uversky · Konstantin K. Turoverov

Received: 15 February 2012 / Accepted: 17 April 2012 / Published online: 17 May 2012

Abstract The studies on the determination of the characteristics of the amyloid fibril interaction with the dye were based on the analysis of the dependence of the ThT fluorescence intensity on its concentration in the solution containing the amyloid fibrils. In the present work, we revealed that this intuitive approach provided erroneous data. We propose a new approach which provides a means for characterizing the interaction of thioflavin T (ThT) with amyloid fibrils and for determining the binding stoichiometry and binding constants, absorption spectrum, molar extinction coefficient, and fluorescence quantum yield of the ThT bound to the sites of different binding modes of fibrils. The key point of this approach is sample preparation by equilibrium microdialysis. The efficiency of the proposed approach is demonstrated via the examination of the ThT binding to insulin and Aβ42 fibrils as well as to the native form of the *Electrophorus electricus* acetylcholinesterase. We show that the peculiarities of ThT interaction with amyloid fibrils depend on the amyloidogenic protein and on the binding mode. This approach is universal and can be used for the analysis of binding mechanism of any dye that interacts with its receptor. Therefore, the proposed approach represents an important addition to the existing arsenal of means for the diagnostics and therapy of the neurodegenerative diseases.

Keywords Thioflavin T · Dye binding · Fluorescence quantum yield · Equilibrium microdialysis · Binding parameters · Amyloid fibrils · Insulin · Aβ42 peptide · Acetylcholinesterase

I. M. Kuznetsova · A. I. Sulatskaya · K. K. Turoverov (✉)
Laboratory of Structural Dynamics, Stability and Folding of Proteins, Institute of Cytology Russian Academy of Sciences,
Tikhoretsky Av. 4,
St. Petersburg 194064, Russia
e-mail: kkt@incras.ru

V. N. Uversky (✉)
Department of Molecular Medicine, College of Medicine,
University of South Florida,
12901 Bruce B. Downs Blvd., MDC07,
Tampa, FL 33612, USA
e-mail: vuversky@health.usf.edu

V. N. Uversky
Institute for Biological Instrumentation,
Russian Academy of Sciences,
142290 Pushchino,
Moscow Region, Russia

Amyloid fibril deposition accompanies several deleterious maladies, such as Alzheimer's and Parkinson's diseases, type II diabetes, and prion diseases [1, 2]. Due to characteristic changes in the fluorescence intensity of the benzothiazole dye thioflavin T (ThT) is frequently used to probe the amyloid fibrils. This approach is based on the unique capability of this dye to form highly fluorescent complexes with amyloid and amyloid-like fibrils [3–5].

The significant increase in the ThT fluorescence intensity in the presence of amyloid fibrils defines the natural intention of the researchers to use this phenomenon as a convenient tool for the characterization of the peculiarities of the ThT interaction with amyloid fibrils (such as the binding constants and binding stoichiometry, number and type of binding sites, number of binding modes, etc.). However, the values of fluorescence intensity of ThT bound to amyloid fibrils formed by different amyloidogenic proteins differ significantly [6, 7]. The cause of this difference is still unclear. It can be determined by the significant difference in the corresponding binding constants and/or by the different fluorescence quantum yields of ThT bound to different amyloid fibrils. Since the fluorescence quantum yield of

ThT in aqueous solution is very low (about 0.0001 [8]), the suggestion that the ThT fluorescence quantum yield increases due to the incorporation of ThT into the amyloid fibril is practically always reasonable. It is obvious that a method for the accurate determination of the fluorescence quantum yield of ThT bound to fibrils is needed. However, until very recently, there were no data on the fluorescence quantum yield of this dye incorporated into amyloid fibrils.

For the first time, such data were obtained for the ThT bound to lysozyme amyloid fibrils which contained sites with different binding modes [9]. Apparently, the lack of data on the fluorescence quantum yield of ThT incorporated into the amyloid fibrils is caused by the fact that the aqueous solutions of ThT in the presence of amyloid fibrils represent a mixture of free and fibril-bound dye, but the accurate evaluation of the concentration of free (bound) dye remained an unsolved issue until recently. The attempt to characterize ThT bound to fibrils was done in several dozens of works, as reviewed by Groenning [10].

Previous studies on the determination of the characteristics of the amyloid fibril interaction with the dye were based on the analysis of the dependence of the ThT fluorescence intensity on its concentration in the solution containing the amyloid fibrils. In the present work, we revealed that this intuitive approach provides erroneous data. The accurate characterization of the dye–fibril interaction can be done using equilibrium microdialysis, a method that was specially designed for the analysis of the small molecule binding to proteins (see e.g., [11]). Surprisingly, this approach was never used for the characterization of ThT binding to amyloid fibrils until now. We also show that samples prepared by this method can be used for the determination of the absorption spectrum of bound dye and for accurate evaluation of the fluorescence quantum yield of ThT bound to fibrils. This became possible after we showed that the recorded fluorescence intensity can be corrected by a factor that depends only on the total optical density of solution and normalized in the units of the product of optical density and fluorescence quantum yield or the sum of such products if there are several modes of the ThT binding to fibrils.

Experimental Procedures

ThT from Sigma (USA) and Fluka (Switzerland) was used after purification by crystallization from a mixture of acetonitrile with ethanol in a 3:1 ratio [12]. ThT "UltraPure Grade" from AnaSpec (USA) was used without additional purification. ThT was dissolved in 2 mM Tris–HCl and 150 mM NaCl buffer (pH 7.7). Fluorescent dye ATTO-425 from ATTO-TEC (Germany); *Electrophorus electricus* acetylcholinesterase (AChE), insulin, and buffer components from Sigma (USA); and Aβ42 peptide from GL Biochem Ltd. (Shanghai, China) were used without additional purification. Insulin amyloid fibrils were produced by the incubation of 10 mg insulin in 1 mL 20 % acetic acid solution in the presence of 100 mM NaCl (pH 2.0) at 37°C at constant stirring [13]. Aβ42 fibrils were prepared by stirring Aβ42 peptide (2 mg/mL) in 50 % hexafluoro-2-propanol (HFIP)/H_2O and 0.02 % sodium azide for 7 days. Afterwards, the HFIP was evaporated under a stream of nitrogen, and the sample was stirred for an additional 7 days [14]. AChE was dissolved in 1 mL 40 mM sodium phosphate buffer at pH 7.0 [15]. Protein concentration was 1.53 mg/mL.

Fluorescence measurements were performed with a homemade spectrofluorimeter [16] and a Cary Eclipse spectrofluorimeter (Varian, Australia). The solution of fluorescent dye ATTO-425 in PBS, whose fluorescence and absorption spectra are similar to that of ThT, was taken as a reference for determining the fluorescence quantum yield of ThT bound to fibrils. Fluorescence of ThT and ATTO-425 was excited at 435 nm and recorded at 480 nm. The spectral slits width was 10 nm in most of experiments. Change of the spectral slits' width did not influence the experimental results. The fluorescence quantum yield of ATTO-425 is 0.9 (ATTO-TEC catalog 2009/2010 p 14).

Equilibrium microdialysis was performed with a Harvard Apparatus/Amika (USA) device, which consists of two chambers (500 μL each) separated by a membrane (MWCO 10,000) impermeable to particles larger than 10,000 Da. Equilibrium microdialysis implies allocation of two interacting agents, a ligand and receptor, in two chambers (#2 and #1, respectively) divided by a membrane permeable to the ligand and impermeable to the receptor (Fig. 1). In our case, the amyloid fibrils in their buffer solutions were placed in chamber #1. The concentration of fibrils in terms of amyloidogenic protein concentration was 0.4 and 0.6 mg/mL for insulin and Aβ42 peptide, respectively. A twofold increase or decrease in fibril concentration did not influence the final results. The ThT solution (in the same buffer as the fibrils placed in chamber #1) with an initial concentration C_0, was placed in chamber #2. After equilibration, the free ThT concentrations in chambers #1 and #2 were equal (C_f), while the total ThT concentration in chamber #1 was greater than that in chamber #2 by the concentration of the bound dye (C_b):

$$C_b = C_0 - 2C_f \quad (1)$$

For performing equilibrium microdialysis, the devices were set on a rocking bar in a thermostatted box for 48 h. All experiments were performed at 23°C. In the test experiments, we put a solution of ThT of concentration C_0 in chamber #2 and the solvent in chamber #1. After 20 h of dialysis, the absorption spectra of samples from chambers #1 and #2 coincide ($D(\lambda)_{\#1} = D(\lambda)_{\#2}$). This means that 24 h

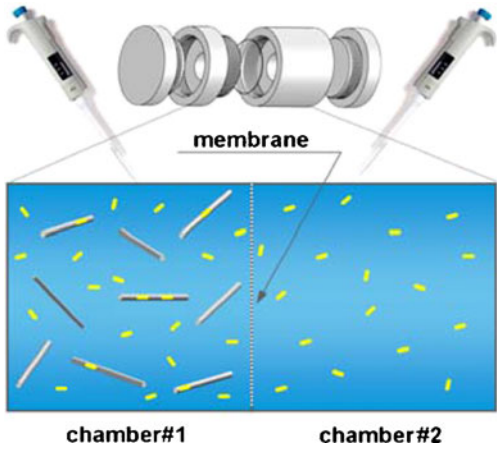

Fig. 1 Principle of equilibrium microdialysis experiment. Device for equilibrium microdialysis represents two chambers (*#2* and *#1*) divided by a membrane permeable to the ligand and impermeable to the receptor. In equilibrium microdialysis experiment, amyloid fibrils in the buffer solution are placed in chamber #1 (concentration of fibrils in terms of amyloidogenic protein concentration is C_p) and the ThT solution in the same buffer is placed in chamber #2 (in concentration C_0). After equilibration, the concentration of free ThT in chambers #1 and #2 become equal (C_f), while the total ThT concentration in chamber #1 become greater than that in chamber #2 by the concentration of the bound dye (C_b): $C_b = C_0 - 2C_f$. Solution in chamber #2 represents the true reference solution for the sample in chamber #1 for spectrophotometric determination of absorption spectrum of dye bound to fibrils

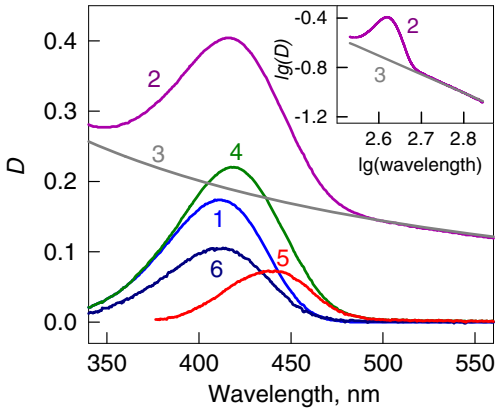

Fig. 2 Absorption spectra of ThT incorporated in the Aβ42 fibrils. Curves *1* and *2* represent absorption spectra of ThT in chamber #1 (free ThT at concentration C_f) and in chamber #2 (superposition of the absorption spectra of free ThT in concentration C_f, ThT bound to fibrils in concentration C_b, and the apparent absorption caused by the light scattering) after the equilibrium attainment. Curve *3* represents optical density determined by the fibril light scattering as calculated by the equation $D_{scat} = a\lambda^{-m}$. Coefficients *a* and *m* were determined from the linear part of the curve *2* (where there is no active dye absorption) plotted in logarithmic coordinates $\lg(D_{scat}) = f(\lg(\lambda))$ (see insert, curve *3*). Curve *4* represents the total absorption of free and bound dyes after light scattering subtraction ($D(\lambda)_{\#2} - D_{scat}$). Curve *5* is the absorption spectra of ThT incorporated in the amyloid fibrils evaluated as $D_b(\lambda) = D(\lambda)_{\#2} - D(\lambda)_{scat} - D(\lambda)_{\#1}$ (the difference between the spectra *4* and *1*). Curve *6* is the absorption spectrum of the free dye at the concentration equal to that of bound dye ($D(\lambda)_0 - 2D(\lambda)_{\#1}$). This curve allows for the evaluation of the change in the molar extinction coefficient of ThT when bound to fibrils

is enough time to allow the dye to equilibrate between chambers #1 and #2. The optical densities of bound dye were determined as described previously [17]. The absorption spectrum of the solution in chamber #1 represents the superposition of the absorption spectra of free ThT in a concentration C_f, ThT bound to fibrils in a concentration C_b ($D_b(\lambda)$), and the apparent absorption determined by light scattered by the fibrils ($D_{scat}(\lambda)$). The dependence of apparent optical density, determined by fibril light scattering, on λ was determined by equation: $D_{scat} = a\lambda^{-m}$. Coefficients *a* and *m* were determined from the linear part of the dependence $D(\lambda)_{\#1}$, where there is no active dye absorption plotted in logarithmical coordinates $\lg(D_{scat}) = f(\lg(\lambda))$. The absorption spectra of ThT incorporated into amyloid fibrils was determined from the equation $D_b(\lambda) = D(\lambda)_{\#1} - D(\lambda)_{scat} - D(\lambda)_{\#2}$ (Fig. 2). The absorption spectra were recorded by spectrophotometer U-3900 H (Hitachi, Japan).

Results

All the experiments were done using the solutions prepared by equilibrium microdialysis as described in "Experimental Procedures". This is a key point of the work since ThT solutions in the presence of amyloid fibrils always contain molecules of free dye, and only equilibrium microdialysis can give a valid set of samples for accurate analysis: the sample solution and the true reference solution to it. For each target amyloid fibril, the equilibrium microdialysis was repeated several times using different input concentrations of ThT. As a result, a large set of solutions with different ThT concentrations was prepared. For each solution, both the absorption spectrum and the fluorescence intensity were recorded. Then obtained experimental data were used for the determination of the ThT–amyloid fibril binding parameters and for the retrieval of the absorption spectrum and the fluorescence quantum yield of ThT bound to fibrils.

Amyloid Fibril–ThT Binding Parameters

If all the ThT binding sites in a target amyloid fibril are identical and independent, then the binding constant of the dye to the amyloid fibril (K_b) is determined as the ratio of the ligand–receptor complex concentration (C_b) to the product of the free receptor (nC_p–C_b) and the free ligand (C_f) concentrations:

$$K_b = \frac{C_b}{(nC_p - C_b)C_f} \quad (2)$$

This means that the dependence of the bound dye concentration on the free dye concentration in solution follows a saturation curve:

$$C_b = \frac{nC_pC_f}{K_d + C_f}. \quad (3)$$

Formerly, other presentations were predominantly popular. The advantage of such presentations is that they linearize the dependence of C_b on C_f, which is a crucial step for the manual determination of binding parameters. Among those representations was the Scatchard plot:

$$\left(\frac{C_b}{C_p}\right)/C_f = nK_b - K_b\left(\frac{C_b}{C_p}\right) \quad (4)$$

and the Klots plot:

$$\frac{1}{C_b} = \frac{1}{nC_p} + \frac{K_d}{nC_p}\frac{1}{C_f} \quad (5)$$

Here, $K_d = 1/K_b$ is the dissociation constant. Based on Eqs. (1) and (2), the dependence of the concentration of bound dye (C_b) on the input dye concentration (C_0) can be calculated as:

$$C_b = \frac{2 + K_bnC_p + K_bC_0 - \sqrt{(2 + K_bnC_p + K_bC_0)^2 - 4K_b^2nC_pC_0}}{2K_b} \quad (6)$$

The value of the binding constant, K_b, and the number of dye binding sites on the fibrils in terms of the protein concentration, n, can be determined on the basis of the experimental dependence of C_b on C_0 (or C_f) by nonlinear regression using appropriate software, e.g., SigmaPlot or GraphPad Prism. Data obtained for AChE could be well described in the frame of the model when all binding sites are identical and independent (i.e., when the interaction process is described by one biding mode) (Fig. 3). This result was quite natural for AChE, which is known to have a single binding site for ThT (n=1) [15].

The failure to find appropriate parameters means that the chosen model does not correspond to the experimental data. In particular, this mismatch can be attributed to the existence of two or more binding modes (i) with different binding constants (K_{bi}). In this case, the binding sites are assumed to be independent from each other, $C_b = \sum_i C_{bi}$, while C_{bi} is characterized by the equations similar to those in Eq. (3). Thus, in the case of i independent modes, we have:

$$C_b = \sum_i \frac{n_iC_pC_f}{K_{di} + C_f} \quad (7)$$

Importantly, in the case of two or more binding modes, the C_{bi} values will not be connected with C_0 by a simple equation similar to Eq. (6).

The nonlinear dependence of C_b on C_f in Scatchard coordinates obtained for ThT binding to insulin and Aβ42 fibrils (Fig. 3), and the failure of Eqs. (2) and (3) to describe the experimental data, suggests that the amyloid fibrils formed by insulin have two or more binding modes. To adequately describe the experimental data, a value of i=2 was assumed, and the values of K_{bi} and n_i were found by fitting the data to Eq. (7) using the GraphPad Prism 5 software. These values are given in Table 1.

Molar Extinction Coefficient of ThT Bound to Amyloid Fibrils

The absorption spectra of solutions obtained for the target objects by the equilibrium microdialysis were recorded. The absorption spectra of ThT bound to amyloid fibrils and AChE were obtained as described in "Experimental Procedures". In the case of one binding mode, the measured absorption spectrum can easily be presented in the units of the molar extinction coefficient:

$$\varepsilon_b(\lambda) = \frac{D_b(\lambda)}{C_b l} \quad (8)$$

In the case of two binding modes, the following equation is true:

$$D_b(\lambda) = D_{b1} + D_{b2} = \varepsilon_{b1}(\lambda)C_{b1}l + \varepsilon_{b2}(\lambda)C_{b2}l \quad (9)$$

Here, $\varepsilon_{b1}(\lambda)$ and $\varepsilon_{b2}(\lambda)$ correspond to the molar extinction coefficients of ThT bound to the binding sites of the

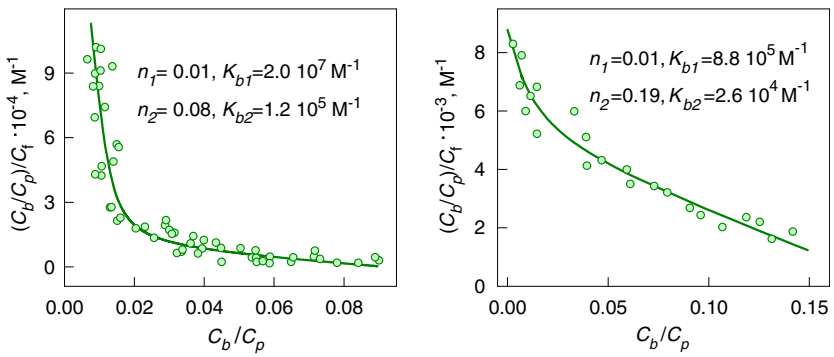

Fig. 3 Scatchard plots for ThT interaction with insulin (*left panel*) and Aβ42 (*right panel*) fibrils. Experimental data (*circles*) and best fit curve with binding constants (K_{bi}) and number of binding sites (n_i) are given on the panels

Table 1 Characteristics of ThT bound to amyloid fibrils, acetylcholinesterase, and free dye in water solution

Object	λ_{max} (nm)	Mode	$\varepsilon_{bi,\max}\times10^{-4}$ (M^{-1} cm^{-1})	$\varepsilon_{bi,435}\times10^{-4}$ (M^{-1} cm^{-1})	$K_{bi}\times10^{-5}$ (M^{-1})	n_i	q_i
Insulin fibrils	450	1	8.7	5.7	200	0.01	0.83
		2	3.5	2.6	1.2	0.08	0.30
Lysozyme fibrils [17]	449	1	5.1	3.7	75	0.11	0.44 [9]
		2	6.7	5.8	0.56	0.24	0.0005 [9]
Aβ42 fibrils	440	1	8.3	8.0	23.80	0.01	0.19
		2	1.8	1.7	0.25	0.21	0.02
Acetylcholinesterase	420	1	2.4	1.9	0.082	1.1	0.036
Thioflavin T in aqueous solution [8]	412	–	3.2	2.0	–	–	0.0001

modes 1 and 2 at wavelength λ. The values of C_{b1} and C_{b2} were determined using Eq. (7) for samples obtained in each equilibrium microdialysis experiment. Figure 4a represents the concentration of ThT, bound with amyloid fibrils as superposition of the concentrations of the dye bound to modes 1 and 2. A large set of the $D_b(\lambda)$, C_{b1}, and C_{b2} values was obtained as a result of the multiple repeats of the equilibrium microdialysis experiments. The $\varepsilon_{b1}(\lambda)$ and $\varepsilon_{b2}(\lambda)$ values can be determined using the known values of $D_b(\lambda)$, C_{b1}, and C_{b2} by multiple linear regressions (e.g., using SigmaPlot). The $\varepsilon_{b1}(\lambda)$ and $\varepsilon_{b2}(\lambda)$ values at the wavelength of fluorescence excitation (435 nm) and at the wavelength of the maximum of bound Th absorption spectrum are given in Table 1.

Similarly, the values of ε_{b1} and ε_{b1} can be determined at the other wavelengths. Figure 4 shows the absorption spectra of the dye bound to the sites of each of two binding modes of insulin and Aβ42 fibrils in units of the molar extinction coefficient. These data show that the molar extinction coefficient of ThT bound to fibrils can depend on the binding mode and can be significantly greater than the molar extinction coefficient evaluated for the free dye in solution (Table 1).

Figure 4c represents the optical density of ThT bound to amyloid fibrils as superposition of optical densities of the dye bound in modes 1 and 2.

Fluorescence Quantum Yield of ThT Bound to Fibrils

For determining the fluorescence quantum yield of ThT bound to amyloid fibrils, the fluorescence intensity was recorded for ThT solution in the presence of amyloid fibrils. Importantly, in these experiments we used the same microdialysis-obtained solutions for which the amyloid fibril–ThT binding parameters (i, n, and K_{bi}) and the absorption spectrum of the bound dye were determined earlier. As these solutions were prepared for different ThT initial concentrations in chamber #2, the dependence of the fluorescence intensity of bound to fibrils dye on optical density was constructed: $I_{ThT} = f(D_b)$.

At the same time, the fluorescence intensity of the solutions of the different concentrations of ATTO-425 was recorded, and the $I_{ATTO} = f(D_{ATTO})$ dependence was plotted. This fluorescent dye was chosen as a standard with known fluorescence quantum yield, since its spectral characteristics (the position of the long wavelength band of absorption spectrum and the fluorescence spectrum position) are similar to those of free ThT in viscous solutions and ThT bound to amyloid fibrils.

The solution of ThT in the presence of amyloid fibrils, which have identical and independent binding sites (i.e., are characterized by one binding mode), is a two-component system in which one component, the free ThT unbound to fibrils, absorbs the excitation light (optical density, D_f) but does not fluoresce, whereas the other component, the ThT bound to fibrils, absorbs the excitation light (optical density, D_b) and fluoresces (quantum yield, q_b). Therefore:

$$I_{ThT} = kI_0\left(1-10^{-(D_b+D_f)}\right)\frac{D_b}{D_b+D_f}\cdot q_b = kI_0\frac{1-10^{-(D_b+D_f)}}{D_b+D_f}D_b\cdot q_b \quad (10)$$

Here, I_0 is the intensity of the excitation light, k is the proportionality coefficient, and $D_b + D_f$ is the total optical density of solution.

If all the binding sites of ThT to fibrils are independent of each other but can be divided into several groups (binding modes) characterized by different binding constants, different binding stoichiometry or different properties of the bound dye (its absorption spectrum, molar extinction coefficient, or fluorescent quantum yield), then Eq. (10) should be rewritten as follows:

$$I_{ThT} = kI_0\frac{1-10^{-(D_b+D_f)}}{D_b+D_f}(D_{b1}q_{b1}+D_{b2}q_{b2}) \quad (11)$$

For simplicity of the presentation, Eq. (11) is given for the case of two binding modes (i=2). For a standard

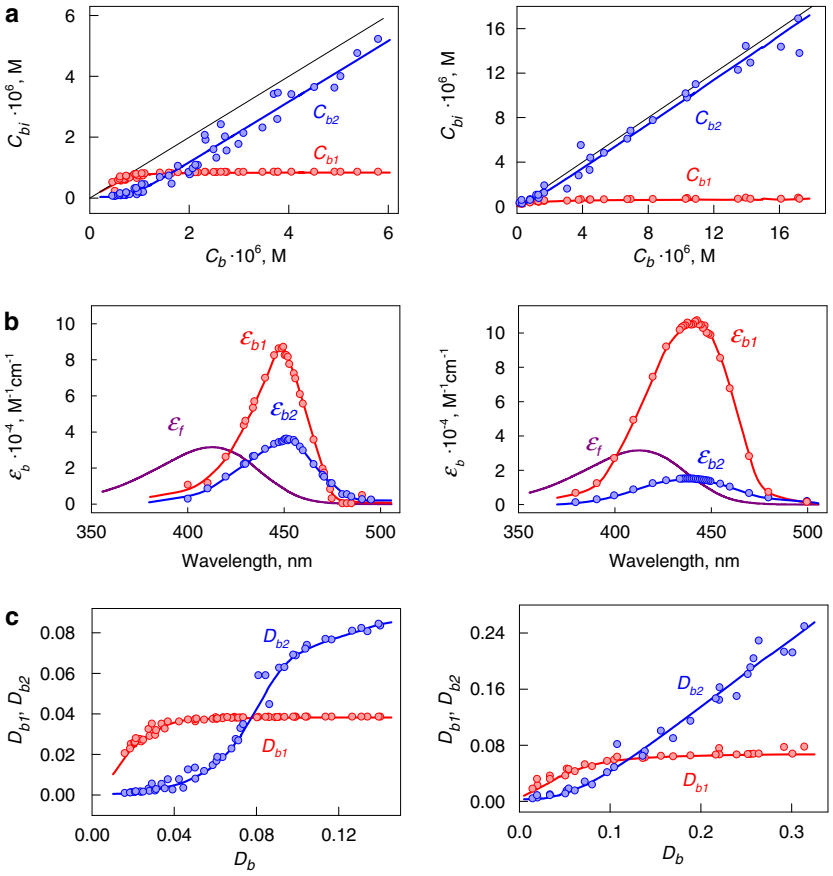

Fig. 4 Determination of the absorption spectra of ThT bound to insulin (*left panels*) and Aβ42 (*right panels*) fibrils. **a** Concentration of ThT, bound with amyloid fibrils (C_b), as superposition of the concentrations of the dye bound to the sites of modes *1* (C_{b1}) and *2* (C_{b2}). **b** Absorption spectra of ThT, bound to the sites of modes *1* and *2* in the units of the molar extinction coefficient. **c** Optical density of ThT bound to amyloid fibrils as superposition of optical densities of the dye bound to the sites of modes *1* (D_{b1}) and *2* (D_{b2})

solution (a solution of the fluorescent dye with known quantum yield, which in our case is the ATTO-425 solution), the equation for fluorescence intensity will be as follows:

$$I_{\mathrm{ATTO}} = kI_0 \frac{1-10^{-D_{\mathrm{ATTO}}}}{D_{\mathrm{ATTO}}} D_{\mathrm{ATTO}} \cdot q_{\mathrm{ATTO}} \qquad (12)$$

In this case, the total optical density of the solution coincides with the optical density of the fluorescent dye. Thus, in the equation for fluorescence intensity three factors can be marked out:

1. The kI_0 factor which depends only on the device used in the experiment. This factor is determined by the intensity of the excitation light, the fluorescence excitation wavelength, the fluorescence registration wavelength, the spectral slits width of the monochromators in the excitation and registration pathways, the photodetector sensitivity, and the peculiarities of signal amplification. Fluorescence intensity is recorded in arbitrary units.
2. The $W_{\mathrm{calc}} = \frac{1-10^{-D_\Sigma}}{D_\Sigma}$ factor which is determined by the total optical density (D_Σ) of solution (at $\lambda = \lambda_{\mathrm{ex}}$) and does not depend on the contribution of fluorescent and nonfluorescent components of solution to the total absorbance. The calculated dependence of this factor on the total optical density of solution $W_{\mathrm{calc}} = f(D_\Sigma)$ is given in Fig. 5a.

The experimental dependence of fluorescence intensity on the optical density of the fluorescent substance can differ from the calculated one (Fig. 5b). The fact that the recorded fluorescence intensity begins to decrease with an increase in the fluorescent substance content, after reaching some value of optical density, is a general property of such dependences and does not indicate the existence of self-quenching or dye aggregation, as it has been frequently suggested (see e.g., [18–20]). In reality, this effect is determined by an increased absorption of excitation light by the solution layers adjacent to the front wall of the spectrofluorimeter cell due to the increase in the total optical density of the solution. The detection system of the spectrofluorimeter "sees" only the central part of the cell, which is reached by a respectively smaller amount of excitation light. Because of this effect, the recorded fluorescence intensity begins to diminish after the optical density reaches a certain value. The effects discussed above depend on the particular instrument used in the experiment and must be taken into account. This can be performed by replacing W_{calc} with an experimentally determined value W.

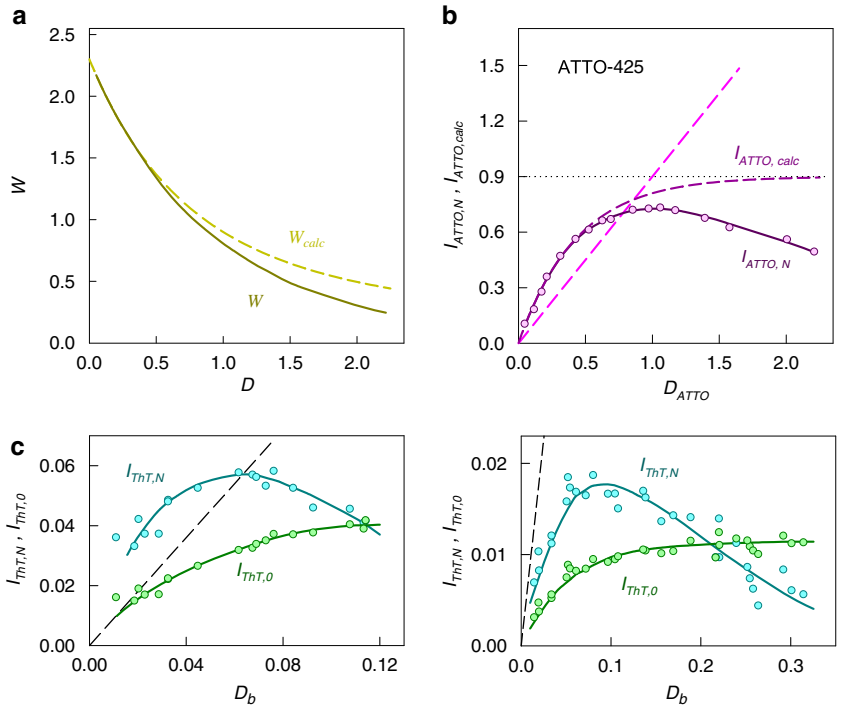

Fig. 5 The dependence of fluorescence intensity on optical density of fluorophore and on total optical density of solution. **a** The dependences $W_{\text{calc}} = \frac{\left(1-10^{-D_{\text{ATTO}}}\right)}{D_{\text{ATTO}}}$ and $W = \frac{I_{\text{ATTO}}/kI_0}{D_{\text{ATTO}} \cdot q_{\text{ATTO}}}$ on total optical density. **b** The dependences of fluorescence intensity on optical density (D^{ATTO}) of the fluorescence dye ATTO-425 with known quantum yield (q_{ATTO}=0.9) calculated as $I_{\text{ATTO,calc}} = \frac{\left(1-10^{-D_{\text{ATTO}}}\right)}{D_{\text{ATTO}}} D_{\text{ATTO}} \cdot q_{\text{ATTO}}$ and experimentally recorded I_{ATTO}. **c** The dependencies of the experimentally recorded fluorescence intensity (I_{ThT}/kI_0) and the reduced fluorescence intensity ($I_{\text{ThT,0}}/W$) of ThT bound to insulin fibrils on its optical density (D_{b}). The straight dashed line is the dependence of $D_{\text{ATTO}} \cdot q_{\text{ATTO}}$ on D_{ATTO} for ATTO-425. **d** The dependencies of the experimentally recorded fluorescence intensity (I_{ThT}/kI_0) and the reduced fluorescence intensity ($I_{\text{ThT,0}}/W$) of ThT bound to Aβ42 fibrils on its optical density (D_{b}). The straight dashed line is the dependence of $D_{\text{ATTO}} \cdot q_{\text{ATTO}}$ on D_{ATTO} for ATTO-425. The details in choosing the normalizing coefficient kI_0 can be seen in the text

The measurement of ATTO-425 fluorescence intensity at different optical density gives an opportunity to determine the dependence of W on total optical density (Fig. 5a) and to choose the normalization coefficient kI_0 in order to correct the fluorescence intensity for the total optical density of solution and to normalize it in the units of the product of optical density and fluorescence quantum yield:

$$kI_0 W = \frac{I_{\text{ATTO}}}{D_{\text{ATTO}} \cdot q_{\text{ATTO}}} \tag{13}$$

In fact, kI_0 must be chosen so that $W \rightarrow W_{\text{calc}}$ at $D_{\text{ATTO}} \rightarrow 0$. In this case, the normalized and corrected fluorescence intensities of ATTO-425 ($I_{\text{ATTO,0}}$) will be defined as:

$$I_{\text{ATTO,0}} = D_{\text{ATTO}} \cdot q_{\text{ATTO}} \tag{14}$$

3. The third factor is the product of optical density and quantum yield of the fluorescent component (in the case of one binding mode) or the sum of the products (in the case of several binding modes). This factor is the only informative element, which bears information on the properties of the fluorescent component(s) in solution. In this case, Eqs. (10) and (11) for normalized and corrected fluorescence intensities ($I_{\text{ThT,0}}$), respectively, will be as follows:

$$I_{\text{ThT,0}} = D_{\text{b}} \cdot q_{\text{b}} \tag{15}$$

$$I_{\text{ThT,0}} = D_{\text{b1}} q_{\text{b1}} + D_{\text{b2}} q_{\text{b2}} \tag{16}$$

Figure 5 represents the dependencies of the ATTO-425 and ThT fluorescence intensities before correction for the total optical density of solution (I_{ATTO}/kI_0 and I_{ThT}/kI_0) and after the corresponding correction ($I_{\text{ATTO,0}}$ and $I_{\text{ThT,0}}$) in the presence of insulin and Aβ42 fibrils. For ATTO-425, the slope of the curve is equal to the q_{ATTO} value. The curves for ThT in the presence of insulin and Aβ42 fibrils are not linear because these fibrils have (at least) two different binding modes of ThT. In this case, the fluorescence quantum yields of ThT bound to the sites of different binding modes can be determined by multiple linear regressions on the basis of Eq. (16), in which the sets of the values $I_{\text{ThT,0}}$, D_{b1}, and D_{b2}

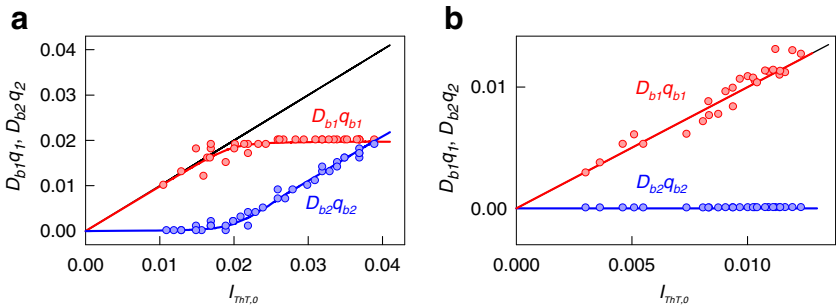

Fig. 6 Corrected and normalized fluorescence intensities of ThT bound to insulin (**a**) and Aβ42 peptide (**b**) amyloid fibrils as superposition of the corrected and normalized fluorescence intensities of the dye bound to the sites of modes *1* ($D_{b1}q_{b1}$) and *2* ($D_{b2}q_{b2}$)

are obtained for solutions prepared by equilibrium microdialysis at different initial ThT concentration, and where the D_{b1} and D_{b2} values are obtained on the basis of C_{b1}, C_{b2}, ε_{b1}, and ε_{b2}. Figure 6 represents the corrected and normalized fluorescence intensities of ThT bound to insulin and Aβ42 peptide amyloid fibrils as superposition of the corrected and normalized fluorescence intensities of the dye bound to the sites of modes 1 and 2.

Discussion

Common Mistakes in the Use of Fluorescence Intensity for the Determination of Binding Parameters

All the currently available data on the parameters of ThT binding to amyloid fibrils which we could find in literature are based solely on the measurements of the ThT fluorescence intensity dependence on the dye concentration in solutions containing amyloid fibrils [10, 15, 21–29]. These analyses are based on the erroneous assumptions that the recorded fluorescence intensity is proportional to the concentration of bound dye ($I = kC_b$) and that the fluorescence intensity plateaus when all binding sites are occupied ($I_{max} = knC_p$) [24]. In the section devoted to the determination of the fluorescence quantum yield of ThT bound to fibrils, we show that both of these assumptions are incorrect, since the fluorescence intensity is proportional to the part of excitation light absorbed by solution, but not to the dye concentration. Even experienced researchers, who do not specialize in fluorescence techniques, do not take into account the fact that a plateau of the fluorescence intensity dependence on the optical density of a fluorescent substance could not point to the saturation of binding centers, since such a "saturable" character of the dependence is its general property.

There is another common mistake in literature regarding the determination of amyloid fibril–ThT binding parameters. Experiments based on the measurement of fluorescence intensity per se cannot, in principle, provide information on the free dye concentration. Nonetheless, researchers used Eqs. (3)–(5) or (7), replacing the value of free dye concentration with the value of input dye concentration, for the determination of the binding constants, without any explanation of such a change (see [3, 24, 25, 29, 30]). This problem was mentioned in the supplement to the work by Sutharsan et al. [30] but was left unsolved. We believe that the replacement of the free dye concentration by the total dye concentration in Eqs. (3)–(5) or (7) contradicts the physical meaning of the model. This mistake was not present in the work by De Ferrari et al. [15] since the dependence of the ThT fluorescence intensity on the C_0 was analyzed using an equation similar to Eq. (6). Nonetheless, the authors of this work still suggested that the fluorescence intensity is proportional to C_b.

Therefore, as of today, we do not know any study where the binding parameters describing the amyloid fibril interaction with ThT or its analogs and derivatives would be determined correctly. In this work, we show how the information on the parameters of ThT binding to fibrils can be obtained if sample and reference solutions are prepared by microdialysis.

Comparative Analysis of ThT Interaction with Different Amyloid Fibrils and Sites of Different Binding Modes of One Type of Amyloid Fibril

The efficiency of the proposed approach is demonstrated by examining the peculiarities of the ThT interaction with insulin and Aβ42 fibrils, as well as with the AChE active center. Sample ThT solutions in the presence of fibrils or AChE and the reference solutions were prepared by equilibrium microdialysis. This step is crucial for the accurate analysis of the ThT binding since it helps to avoid the mistakes associated with the use of fluorescence intensity for the determination of binding parameters, given that of the three factors in determining fluorescence intensity, only one contains information on the fluorescence substance, namely, the product of its optical density and fluorescence quantum yield (see above).

Registration of the absorption spectra of the solutions containing the target amyloid fibrils and ThT in different concentrations gave us a set of data for the determination of binding constants and stoichiometry of ThT interaction with target amyloid fibrils, together with the absorption spectrum

of ThT in the bound state. Then, registration of the fluorescence intensity for the same solutions, combined with the knowledge of the binding parameters, allowed for the determination of the fluorescence quantum yield of ThT bound to fibrils. All the binding parameters obtained for the ThT interaction with the insulin and Aβ42 fibrils, as well as with the AChE active center, are summarized in Table 1.

The experimental data for the ThT binding to the amyloid fibrils are fitted well by the simplest model, according to which ThT incorporates in amyloid fibrils in the monomeric form, and all the binding sites are independent of each other. This agrees with the Krebs model of ThT binding to amyloid fibrils [31], which suggested that the dye is inserted in grooves that run along the length of the β-sheet. Later, this model of ThT interaction with amyloid was supported by the molecule dynamics simulations [32–34] and the near-field scanning optical microscopy [35].

For all the amyloid and amyloid-like fibrils analyzed in our study, two binding modes were found (Table 1). Binding constants of these two modes differ by two orders of magnitude. All n_i for amyloid fibrils are significantly lower than 1. This means that the ThT binding to fibrils cannot be described by the 1:1 stoichiometry, and instead, the formation of one ThT binding site requires $(1/n_i)$ amyloidogenic protein or peptide molecules.

In the case of AChE, the stoichiometry is 1:1, suggesting that this protein has one active center which is able to bind to just one ThT molecule. The value of the ThT–AChE binding constant is lower than the lowest values of the ThT–insulin and ThT–lysozyme binding constants and is comparable with that of the ThT–Aβ42 fibrils. These observations correlate with the relatively small red shift of absorption spectrum of ThT bound to AChE in comparison with that of free ThT in aqueous solution and low fluorescence quantum yield (see Table 1).

The significantly shorter wavelength position of the absorption spectrum of free ThT in solution, in comparison to that of ThT incorporated into amyloid fibrils, can be explained by the orientational dipole–dipole interaction of the dye molecules with a polar solvent. In reality, the ThT ground state is stabilized by the orientational interactions of the polar solvent dipoles with the dipole caused by the positive charge of the ThT molecule, which is unequally distributed between the benzothiazole and aminobenzoyl rings, while the configuration of the solvation shell of the ThT molecule in the excited Franck–Condon state is far from being in equilibrium (see [36, 37]). The ThT absorption spectrum has the shortest wavelengths maximum in water (412 nm), while the absorption spectra of ThT bound to amyloid fibrils are red-shifted with maxima at 450, 440, and 449 nm for the insulin, Aβ42, and lysozyme, respectively [17].

ThT binding to fibrils is accompanied not only by a significant red shift of the absorption spectrum but also by a significant change in the molar extinction coefficient of the dye. This result agrees with the quantum chemical simulations that predicted the dependence of the value of the oscillator strength corresponding to the ThT transition from the ground to the excited state on the φ value between the benzothiazole and aminobenzoyl rings [38] and with the assumption that the conformation of ThT molecules bound to amyloid fibrils may differ from that of free molecule in solution [8]. The molar extinction coefficient of ThT bound to AChE is similar to that of free ThT in aqueous solution, whereas the molar extinction coefficients of ThT bound to fibrils are noticeably larger.

Using the value of optical density and the fluorescence data, the fluorescence quantum yield of the ThT bound to fibrils in each binding mode can be determined (Table 1). As was predicted [8], the fluorescence quantum yield of ThT incorporated into amyloid fibrils depends not only on the restriction of the ThT benzothiazole and aminobenzoyl rings' mobility against each other in the excited state but also on the molecular conformation of ThT in the ground state and could be both larger or smaller than quantum yield in rigid isotropic solution (q=0.28). We show here that in the case of insulin fibrils, the binding of ThT is characterized by the highest binding constants, and the insulin fibril-bound ThT possesses the highest fluorescence quantum yield (q_{b1}=0.83).

Conclusions

The obtained results show that the use of the equilibrium microdialysis opens new perspectives for the ThT application in investigation of the amyloid fibril structure. The proposed approach is universal for determining the binding parameters of any dye to any receptor. We hypothesize that this tool can be implemented in experiments of the accurate evaluation of the binding parameters of the neutral ThT analogs (which can penetrate the hematoencephalic barrier) to amyloid fibrils. This may also have impact on the successful development of diagnosis and therapy of neurodegenerative diseases [27, 29, 30, 39–42].

Acknowledgments This work was supported in part by the "Molecular and Cell Biology" Program of the Russian Academy of Sciences (KKT and VNU); Russian Foundation of Basic Research, grants #12-04-01651 (KKT) and #12-04-90022_Bel (KKT); and Dmitry Zimin's Russian Charitable Foundation "Dynasty" (AIS). We are extremely grateful to Alexey V. Uversky for careful reading and editing this manuscript.

References

1. Dobson CM (1999) Protein misfolding, evolution and disease. Trends Biochem Sci 24(9):329–332
2. Dobson CM (2003) Protein folding and misfolding. Nature 426 (6968):884–890

3. LeVine H 3rd (1993) Thioflavine T interaction with synthetic Alzheimer's disease beta-amyloid peptides: detection of amyloid aggregation in solution. Protein Sci 2(3):404–410
4. LeVine H 3rd (1999) Quantification of beta-sheet amyloid fibril structures with thioflavin T. Methods Enzymol 309:274–284
5. Naiki H, Higuchi K, Hosokawa M, Takeda T (1989) Fluorometric determination of amyloid fibrils in vitro using the fluorescent dye, thioflavin T1. Anal Biochem 177(2):244–249
6. Tycko R (2011) Solid-state NMR studies of amyloid fibril structure. Annu Rev Phys Chem 62:279–299
7. Tycko R (2004) Progress towards a molecular-level structural understanding of amyloid fibrils. Curr Opin Struct Biol 14 (1):96–103
8. Sulatskaya AI, Kuznetsova IM, Maskevich AA, Uversky VN, Turoverov KK (2010) Non-radiative deactivation of the excited state of thioflavin T: dependence on solvent viscosity and temperature. PLoS One 5(10):e15385
9. Sulatskaya AI, Kuznetsova IM, Turoverov KK (2012) Interaction of thioflavin T with amyloid fibrils: fluorescence quantum yield of bound dye. J Phys Chem B 116(8):2538–2544
10. Groenning M (2010) Binding mode of Thioflavin T and other molecular probes in the context of amyloid fibrils-current status. J Chem Biol 3(1):1–18
11. Oravcova J, Bohs B, Lindner W (1996) Drug–protein binding sites. New trends in analytical and experimental methodology. J Chromatogr B Biomed Appl 677(1):1–28
12. Voropay ES, Samtsov MP, Kaplevsky KN, Maskevich AA, Stepuro VI, Povarova OI, Kuznetsova IM, Turoverov KK, Fink AL, Uversky VN (2003) Spectral properties of Thioflavin T and its complexes with amyloid fibrils. J Appl Spectrosc 70(6):868–874
13. Goers J, Permyakov SE, Permyakov EA, Uversky VN, Fink AL (2002) Conformational prerequisites for alpha-lactalbumin fibrillation. Biochemistry 41(41):12546–12551
14. Kayed R, Head E, Sarsoza F, Saing T, Cotman CW, Necula M, Margol L, Wu J, Breydo L, Thompson JL, Rasool S, Gurlo T, Butler P, Glabe CG (2007) Fibril specific, conformation dependent antibodies recognize a generic epitope common to amyloid fibrils and fibrillar oligomers that is absent in prefibrillar oligomers. Mol Neurodegener 2:18
15. De Ferrari GV, Mallender WD, Inestrosa NC, Rosenberry TL (2001) Thioflavin T is a fluorescent probe of the acetylcholinesterase peripheral site that reveals conformational interactions between the peripheral and acylation sites. J Biol Chem 276 (26):23282–23287
16. Turoverov KK, Biktashev AG, Dorofeiuk AV, Kuznetsova IM (1998) A complex of apparatus and programs for the measurement of spectral, polarization and kinetic characteristics of fluorescence in solution. Tsitologiia 40(8–9):806–817
17. Sulatskaya AI, Kuznetsova IM, Turoverov KK (2011) Interaction of thioflavin T with amyloid fibrils: stoichiometry and affinity of dye binding, absorption spectra of bound dye. J Phys Chem B 115 (39):11519–11524
18. Dzwolak W, Pecul M (2005) Chiral bias of amyloid fibrils revealed by the twisted conformation of Thioflavin T: an induced circular dichroism/DFT study. FEBS Lett 579(29):6601–6603
19. Uversky VN, Winter S, Lober G (1996) Use of fluorescence decay times of 8-ANS-protein complexes to study the conformational transitions in proteins which unfold through the molten globule state. Biophys Chem 60(3):79–88
20. Uversky VN, Winter S, Lober G (1998) Self-association of 8-anilino-1-naphthalene-sulfonate molecules: spectroscopic characterization and application to the investigation of protein folding. Biochim Biophys Acta 1388:133–142
21. Groenning M, Norrman M, Flink JM, van de Weert M, Bukrinsky JT, Schluckebier G, Frokjaer S (2007) Binding mode of Thioflavin T in insulin amyloid fibrils. J Struct Biol 159(3):483–497
22. Groenning M, Olsen L, van de Weert M, Flink JM, Frokjaer S, Jorgensen FS (2007) Study on the binding of Thioflavin T to beta-sheet-rich and non-beta-sheet cavities. J Struct Biol 158(3):358–369
23. Fodera V, Groenning M, Vetri V, Librizzi F, Spagnolo S, Cornett C, Olsen L, van de Weert M, Leone M (2008) Thioflavin T hydroxylation at basic pH and its effect on amyloid fibril detection. J Phys Chem B 112(47):15174–15181
24. Morimoto K, Kawabata K, Kunii S, Hamano K, Saito T, Tonomura B (2009) Characterization of type I collagen fibril formation using thioflavin T fluorescent dye. J Biochem 145(5):677–684
25. Sabate R, Lascu I, Saupe SJ (2008) On the binding of Thioflavin-T to HET-s amyloid fibrils assembled at pH 2. J Struct Biol 162 (3):387–396
26. LeVine H 3rd (1997) Stopped-flow kinetics reveal multiple phases of thioflavin T binding to Alzheimer beta (1–40) amyloid fibrils. Arch Biochem Biophys 342(2):306–316
27. Lockhart A, Ye L, Judd DB, Merritt AT, Lowe PN, Morgenstern JL, Hong G, Gee AD, Brown J (2005) Evidence for the presence of three distinct binding sites for the thioflavin T class of Alzheimer's disease PET imaging agents on beta-amyloid peptide fibrils. J Biol Chem 280(9):7677–7684
28. Ye L, Morgenstern JL, Gee AD, Hong G, Brown J, Lockhart A (2005) Delineation of positron emission tomography imaging agent binding sites on beta-amyloid peptide fibrils. J Biol Chem 280(25):23599–23604
29. Ye L, Velasco A, Fraser G, Beach TG, Sue L, Osredkar T, Libri V, Spillantini MG, Goedert M, Lockhart A (2008) In vitro high affinity alpha-synuclein binding sites for the amyloid imaging agent PIB are not matched by binding to Lewy bodies in postmortem human brain. J Neurochem 105(4):1428–1437
30. Sutharsan J, Dakanali M, Capule CC, Haidekker MA, Yang J, Theodorakis EA (2010) Rational design of amyloid binding agents based on the molecular rotor motif. Chem Med Chem 5(1):56–60
31. Krebs MR, Bromley EH, Donald AM (2005) The binding of thioflavin-T to amyloid fibrils: localisation and implications. J Struct Biol 149(1):30–37
32. Wu C, Biancalana M, Koide S, Shea JE (2009) Binding modes of thioflavin-T to the single-layer beta-sheet of the peptide self-assembly mimics. J Mol Biol 394(4):627–633
33. Biancalana M, Koide S (2010) Molecular mechanism of Thioflavin-T binding to amyloid fibrils. Biochim Biophys Acta 1804(7):1405–1412
34. Biancalana M, Makabe K, Koide A, Koide S (2009) Molecular mechanism of thioflavin-T binding to the surface of beta-rich peptide self-assemblies. J Mol Biol 385(4):1052–1063
35. Kitts CC, Vanden Bout DA (2009) Near-field scanning optical microscopy measurements of fluorescent molecular probes binding to insulin amyloid fibrils. J Phys Chem B 113(35):12090–12095
36. Turoverov KK, Kuznetsova IM, Maskevich AA, Stepuro VI, Kuzmitsky VA, Uversky VN (2007) ThT as an instrument for testing and investigation of amyloid and amyloid-like fibrils. Proc SPIE 6733:1–7
37. Maskevich AA, Stsiapura VI, Kuzmitsky VA, Kuznetsova IM, Povarova OI, Uversky VN, Turoverov KK (2007) Spectral properties of thioflavin T in solvents with different dielectric properties and in a fibril-incorporated form. J Proteome Res 6(4):1392–1401
38. Stsiapura VI, Maskevich AA, Kuzmitsky VA, Turoverov KK, Kuznetsova IM (2007) Computational study of thioflavin T torsional relaxation in the excited state. J Phys Chem A 111 (22):4829–4835
39. Klunk WE, Wang Y, Huang GF, Debnath ML, Holt DP, Shao L, Hamilton RL, Ikonomovic MD, DeKosky ST, Mathis CA (2003) The binding of 2-(4′-methylaminophenyl)benzothiazole to post-mortem brain homogenates is dominated by the amyloid component. J Neurosci 23(6):2086–2092

40. Mathis CA, Wang Y, Holt DP, Huang GF, Debnath ML, Klunk WE (2003) Synthesis and evaluation of 11 C-labeled 6-substituted 2-arylbenzothiazoles as amyloid imaging agents. J Med Chem 46 (13):2740–2754
41. Henriksen G, Hauser AI, Westwell AD, Yousefi BH, Schwaiger M, Drzezga A, Wester HJ (2007) Metabolically stabilized benzothiazoles for imaging of amyloid plaques. J Med Chem 50(6):1087–1089
42. Ono M (2009) Development of positron-emission tomography/single-photon emission computed tomography imaging probes for in vivo detection of beta-amyloid plaques in Alzheimer's brains. Chem Pharm Bull (Tokyo) 57(10):1029–1039